

Stereoselective Synthesis of Unnatural α -Amino Acids through Photoredox Catalysis

Andrey Shatskiy,[†] Anton Axelsson,[†] Björn Blomkvist,[†] Jian-Quan Liu,[†] Peter Dinér,[†] and Markus D. Kärkäs^{*†}

[†] Department of Chemistry, KTH Royal Institute of Technology, SE-100 44 Stockholm, Sweden

Abstract

A protocol for stereoselective C-radical addition to a chiral glyoxylate-derived sulfinyl imine was developed through visible light-promoted photoredox catalysis, providing a convenient method for the synthesis of unnatural α -amino acids. The developed protocol allows the use of ubiquitous carboxylic acids as radical precursors without prior derivatization. The protocol utilizes near-stoichiometric amounts of the imine and the acid radical precursor in combination with a catalytic amount of an organic acridinium-based photocatalyst. The mechanism for the developed transformation is discussed and the stereodetermining radical addition step was studied by the DFT calculations.

Keywords: *amino acids, carboxylic acids, decarboxylation, organic photocatalyst, photoredox catalysis, stereoselective synthesis*

Introduction

Unnatural α -amino acids constitute an important class of biologically relevant compounds that are widely used in both pharmaceutical industry and fundamental research.¹ A number of pharmaceuticals based on unnatural α -amino acids are currently on the market, including ACE inhibitors for the treatment of cardiovascular and renal diseases,² antiviral medicines,³ and others.⁴ Most recently, several drug target studies addressing the globally threatening respiratory disease COVID-19 caused by the SARS-CoV-2 coronavirus were released.⁵ Therein, a number of unnatural α -amino acid-based drug candidates were identified, in particular peptidomimetic α -ketoamide inhibitors, demonstrating the high demand for such building blocks in the present time.

A variety of synthetic strategies to access unnatural amino acid derivatives have been developed over the years, with some notable methods being the catalytic asymmetric Strecker-type reactions, asymmetric hydrogenation of dehydroamino acids, and electrophilic and nucleophilic alkylation of glycine derivatives (Figure 1).⁶ Among these, functionalization or reduction of α -imino esters offers a straightforward route to various enantiomerically enriched α -amino acids.⁷ Traditionally, these strategies have employed polar retrosynthetic disconnections, which often require the use of (super)stoichiometric amounts of toxic and highly sensitive reagents at low temperatures, thereby limiting the substrate scope and practicality for scale up of these reactions. These limitations have recently been challenged by re-introduction of free radical reaction manifolds, aided by developments in base-metal catalysis,⁸ electrocatalysis⁹ and photoredox catalysis.¹⁰ Radical addition to imines through photoredox catalysis was recently demonstrated in symmetric¹¹ and asymmetric¹² fashion. In 2017, Alemán and co-workers reported a protocol for asymmetric radical addition to imines mediated by visible light.¹² The developed catalytic system made use of a chiral sulfoxide auxiliary group, commonly employed in the synthesis of chiral amines.¹³ Here, the C-centered radical was generated through visible light-mediated reductive cleavage of the N–O bond in a redox-active phthalimide ester, followed by radical addition to the sulfinyl imine. The reductive nature of the

protocol necessitates a stoichiometric amount of a reducing agent (Hantzsch ester) to be used. More recently, a related Ni-based catalytic system was described by Baran and co-workers.¹⁴ This protocol also employed a redox-active ester as the radical precursor, with Zn as a stoichiometric reducing agent and a Ni-based catalyst for mediating the C–C bond formation. Although this protocol displayed an impressive substrate scope, it is associated with moderate atom-economy, limiting its applicability for large-scale synthesis.

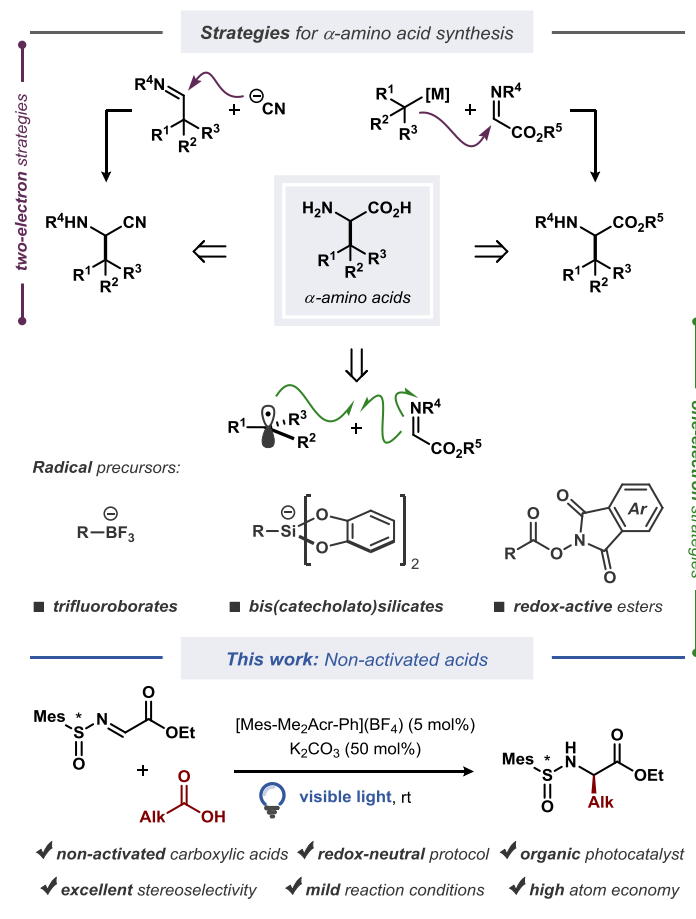


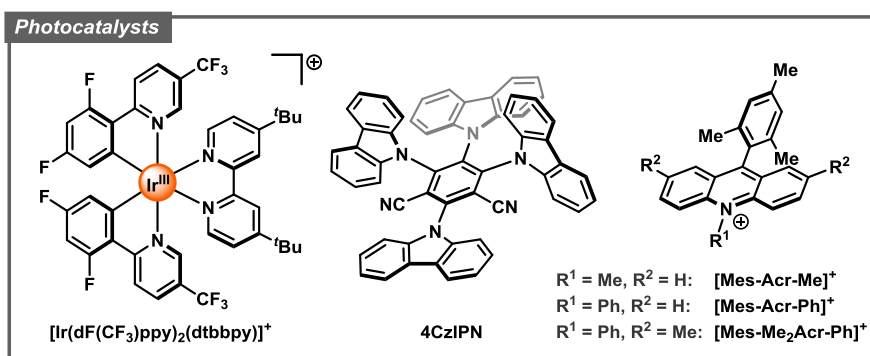
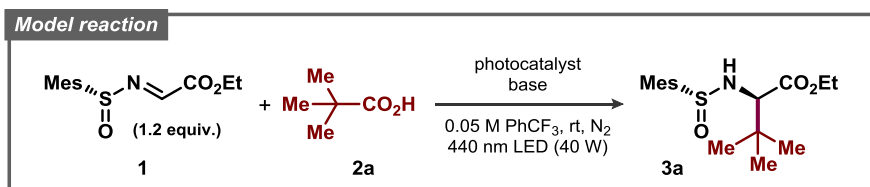
Figure 1. Strategies for synthesis of unnatural α -amino acids (top), and diastereoselective decarboxylative alkylation of sulfinyl imines with non-activated carboxylic acids (bottom).

Results and Discussion

Inspired by the catalytic systems developed by the Alemán,¹² Ye,^{11a} and Baran¹³ groups, we sought to realize a protocol for diastereoselective decarboxylative radical addition to chiral sulfinyl imines that

would utilize ubiquitous non-activated carboxylic acids as radical precursors.¹⁵ A related direct decarboxylative addition process was attempted by the Alemán group for a benzaldehyde-derived sulfinyl imine under reaction conditions reported by MacMillan,¹⁶ however, no formation of the desired product was observed (see the Supporting Information to ref. 12). Similarly, we observed no desired product with pivalic acid **2a** as the radical precursor and sulfinyl imine **1** as the radical acceptor when the reaction was conducted in DMSO with [Ir(dF(CF₃)ppy)₂(dtbbpy)](PF₆) as photocatalyst (Table 1, entry 1), presumably due to fast decomposition of sulfinyl imine **1**. Gratifyingly, changing the solvent to α,α,α -trifluorotoluene (PhCF₃) furnished the desired product **3a** in fairly good yield of 65%, although with poor diastereoselectivity (Table 1, entry 2). Using other bases in place of Cs₂CO₃ completely prohibited the reaction (for details on the optimization studies, see the Supporting Information), and the highly-oxidizing photocatalyst 4CzIPN¹⁷ failed to deliver the radical addition product (Table 1, entry 3). Fortunately, the highly-oxidizing organic acridinium-based photocatalyst [Mes-Acr-Me](BF₄) delivered product **3a** with excellent diastereoselectivity, although in poor yield (Table 1, entry 4). Increasing the catalyst loading from 1 to 5 mol% and switching to the more stable *N*-phenyl-substituted photocatalysts [Mes-Acr-Ph](BF₄) and [Mes-Me₂Acr-Ph](BF₄)¹⁸ dramatically increased the yield of the stereoselective radical addition product up to 78% (Table 1, entries 5–7). Changing the base to K₂CO₃ and increasing the base loading further improved the yield up to 85% (Table 1, entry 11). Finally, utilizing a slight excess of the acid radical precursor **2a** delivered the desired product **3a** in excellent yields (91% and 95% for 1.2 and 1.5 equiv. of **2a**, respectively; Table 1, entries 13 and 14). Consistently with the previous reports on radical additions to sulfinyl imines, the *tert*-butyl- and *para*-tolyl-substituted sulfinyl imines **4** and **5** proved to be inefficient as radical acceptors (Table 1, entries 15 and 16).^{12,14} In case of *tert*-butyl-substituted sulfinyl imine **4**, it is likely that the transiently formed

Table 1. Optimization of the reaction conditions for the decarboxylative radical addition to a glyoxylate-derived sulfinyl imine.^a



entry	photocatalyst	base	time	yield ^b	dr ^b
1 ^c	$[\text{Ir}(\text{dF}(\text{CF}_3)\text{ppy})_2(\text{dtbbpy})](\text{PF}_6)$, 1 mol%	Cs ₂ CO ₃ , 0.2 equiv.	20 min	< 5%	—
2	$[\text{Ir}(\text{dF}(\text{CF}_3)\text{ppy})_2(\text{dtbbpy})](\text{PF}_6)$, 1 mol%	Cs ₂ CO ₃ , 0.2 equiv.	20 min	65%	4 : 1
3	4CzIPN, 1 mol%	Cs ₂ CO ₃ , 0.2 equiv.	20 min	< 5%	—
4	$[\text{Mes-Acr-Me}](\text{BF}_4)$, 1 mol%	Cs ₂ CO ₃ , 0.2 equiv.	20 min	27%	> 95 : 5
5	$[\text{Mes-Acr-Me}](\text{BF}_4)$, 5 mol%	Cs ₂ CO ₃ , 0.2 equiv.	20 min 60 min	48% 66%	> 95 : 5 > 95 : 5
6	$[\text{Mes-Acr-Ph}](\text{BF}_4)$, 5 mol%	Cs ₂ CO ₃ , 0.2 equiv.	60 min	73%	> 95 : 5
7	$[\text{Mes-Me}_2\text{Acr-Ph}](\text{BF}_4)$, 5 mol%	Cs ₂ CO ₃ , 0.2 equiv.	60 min	78%	> 95 : 5
8	$[\text{Mes-Me}_2\text{Acr-Ph}](\text{BF}_4)$, 5 mol%	K ₃ PO ₄ , 0.2 equiv.	60 min	80%	> 95 : 5
9	$[\text{Mes-Me}_2\text{Acr-Ph}](\text{BF}_4)$, 5 mol%	K ₂ CO ₃ , 0.2 equiv.	60 min	84%	> 95 : 5
10	$[\text{Mes-Me}_2\text{Acr-Ph}](\text{BF}_4)$, 5 mol%	K ₂ CO ₃ , 0.05 equiv.	20 min	< 5%	—
11	$[\text{Mes-Me}_2\text{Acr-Ph}](\text{BF}_4)$, 5 mol%	K ₂ CO ₃ , 0.5 equiv.	60 min	85%	> 95 : 5
12 ^d	$[\text{Mes-Me}_2\text{Acr-Ph}](\text{BF}_4)$, 5 mol%	K ₂ CO ₃ , 0.5 equiv.	60 min	77%	> 95 : 5
13 ^e	$[\text{Mes-Me}_2\text{Acr-Ph}](\text{BF}_4)$, 5 mol%	K ₂ CO ₃ , 0.5 equiv.	60 min	91%	> 95 : 5
14 ^f	$[\text{Mes-Me}_2\text{Acr-Ph}](\text{BF}_4)$, 5 mol%	K ₂ CO ₃ , 0.5 equiv.	60 min	95%	> 95 : 5
15	As entry 13, but with ^t Bu-sulfinyl imine 4		60 min	< 5%	—
16	As entry 13, but with <i>p</i> -Tol-sulfinyl imine 5		60 min	50%	7 : 1
deviations from the conditions in entry 13					
17	under air		60 min	12%	> 95 : 5
18	no photocatalyst		60 min	< 5%	—
19	no light		60 min	< 5%	—

^a The reactions were performed on 0.1 mmol scale: stock solutions of the pivalic acid **2** and the photocatalyst (each in 1 mL of the solvent) were mixed with the sulfinyl imine **1** and the base under anhydrous conditions, and stirred under irradiation with 440 nm blue LED light at room temperature (for details, see the Supporting Information).

^b Determined by ¹H NMR of a crude reaction mixture with 1,3,5-trimethoxybenzene as an internal standard. ^c 0.1 M DMSO.

^d 0.1 M PhCF₃. ^e 1.0 equiv. of sulfinyl imine **1** and 1.2 equiv. of pivalic acid **2**. ^f 1.0 equiv. of sulfinyl imine **1** and 1.5 equiv. of pivalic acid **2**.

aminyl radical intermediate underwent decomposition to form an iminosulfanone ($-N=S=O$), thereby disrupting the catalytic cycle.¹⁹

The substrate scope of the developed transformation was evaluated with a variety of commercially available tertiary, secondary, and primary carboxylic acids (Figure 2). For all of the amino acid derivatives, except product **3f**, excellent diastereoselectivity at the α -position was observed ($>95:5$ *dr*). The unfunctionalized tertiary carboxylic acids **2a** and **2c** delivered the radical addition products **3a** and **3c** in high yields (81% and 87%, respectively). The potentially oxidatively sensitive gemfibrozil-derived product **3b** could also be accessed, although in lower yield (44%). Surprisingly, *N*-Boc-piperidine-derived product **3d** was obtained in relatively low yield (33%), while oxetane- and cyclopropyl-containing carboxylic acids **2e** and **2f** delivered the corresponding products **3e** and **3f** in moderate yields (54% and 52%, respectively). The cyclohexyl radical addition adduct **3h** was obtained in high yield (73%), while other non-stabilized secondary and primary carboxylic acids **2l–k** provided lower yields compared to the tertiary acids, consistent with previous reports featuring secondary and primary free radical intermediates under related conditions.²⁰ Further optimization of the reaction conditions for the primary acids **2j** and **2k** did not result in improved yields (Tables S2 and S3), illustrating the intrinsic instability of the respective radical intermediates and/or the photocatalyst under the employed conditions.

Next, we surveyed carboxylic acid radical precursors that furnish stabilized α -heteroatom C-radicals. Gratifyingly, *N*-Boc-protected α -amino acid radical precursors based on pipecolic acid, proline, valine, and phenylalanine provided the expected amino acid derivatives **3l–o** in generally excellent yields (up to $>99\%$), exemplifying a prominent synthetic route to biologically active α,β -diamino acids.²¹ The α -*O*-substituted radicals derived from tetrahydro-2-furonic and methoxymandelic acids provided the expected radical addition products **3p** and **3q** in 45% and 60% yields, respectively. A tertiary α -*O*-substituted radical derived from clofibric acid **2g** delivered product **3g** in excellent yield (90%). Interestingly, products **3n–q** were obtained not only with

excellent diastereoselectivity at the α -position (>95:5 *dr*), but also with a slight diastereoselectivity at the β -position (up to 1.5:1 *dr*). In general, the acids with strong electron-withdrawing substituents at the α -position (CF_3 , benzyl, and benzoyl) did not provide the desired products, likely due to the insufficient nucleophilic character of the formed C-radicals (see the unsuccessful substrates in Figure 2). The α -H and α -Me-substituted cyclopropanecarboxylic acids were also inefficient, despite successful reaction with the analogous α -Ph-substituted substrate **2f**.

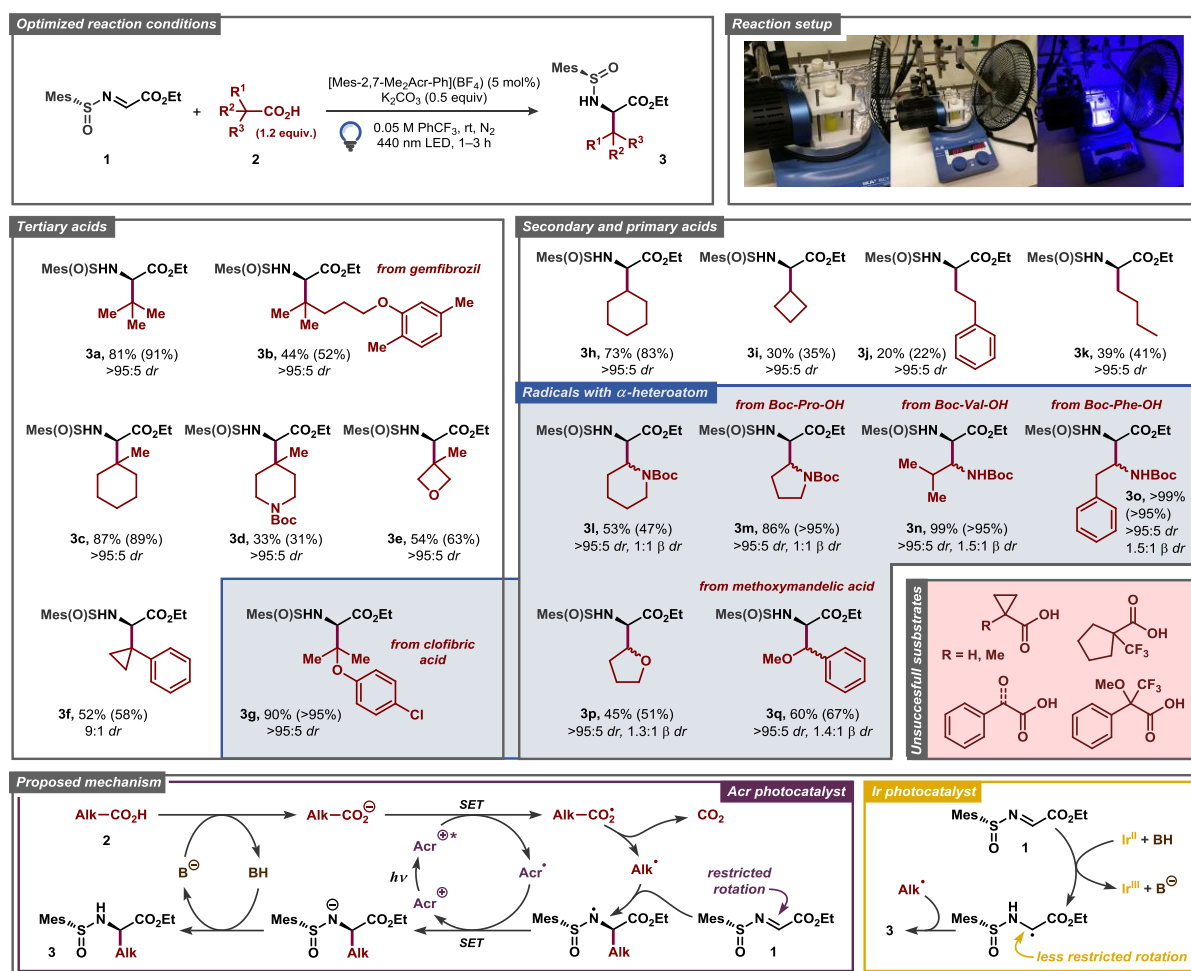


Figure 2. Substrate scope for the decarboxylative radical addition to glyoxylate-derived sulfinyl imine **1** to furnish the unnatural amino acid precursors **3**. The isolated yields of the products and NMR-yields from the crude reaction mixtures (in parenthesis) are reported (see the Supporting Information for details). ^a 1 mmol scale reaction.

Based on previous literature precedents, a mechanism for the developed transformation was proposed (Figure 2, bottom).^{12,22} Initially, the acridinium photocatalyst [Mes-Me₂Acr-Ph](BF₄) (Acr⁺) is excited by visible light ($\lambda_{\text{max}} \approx 425$ nm) to a highly oxidizing excited state Acr^{+*} ($E(\text{Acr}^{+*}/\text{Acr}^{\bullet}) \approx 2.09$ V vs. SCE).²³ In this state, the photocatalyst can abstract an electron from the deprotonated carboxylic acid *via* a single-electron transfer (SET) event to generate a carboxylate radical while being reduced to the acridinium radical Acr[•]. The carboxyl radical then extrudes CO₂ to form a C-centered radical, which undergoes addition to the sulfinyl imine **1** in the key step of the reaction, forming an α -alkylated *N*-centered radical. Finally, the *N*-centered radical is reduced by Acr[•], closing the photocatalytic cycle and furnishing the desired product **3** upon protonation.

An alternative mechanism for a related radical addition process to imine derivatives was proposed by Ooi and co-workers.²⁴ Here, the key C–C bond-forming step was found to proceed through radical-radical coupling between a C-centered radical and an azaketyl-type radical. However, under our conditions such a mechanistic pathway seems unlikely due to weak reducing ability of the one-electron reduced form of the employed acridinium photocatalyst ($E(\text{Acr}^+/\text{Acr}^{\bullet}) \approx -0.58$ V vs. SCE). As opposed to the conditions reported by Ooi and co-workers, where strongly reducing [Ir(ppy)₂(bpy)]⁺-type photocatalysts ($E(\text{Ir}^{\text{III}}/\text{Ir}^{\text{II}}) \approx -1.5$ V vs. SCE) were used, electron transfer from Acr[•] to sulfinyl imine **1** ($E_p \approx -1.1$ V vs. SCE, as determined by cyclic voltammetry) should not be favored. Notably, a shift to an Ooi-type radical-radical coupling pathway could explain the low diastereoselectivity (4:1 *dr*) during formation of product **3a** when the reaction was conducted with the [Ir(dF(CF₃)ppy)₂(dtbbpy)](PF₆) photocatalyst (Table 1, entry 2; Figure 2, bottom right). The low diastereoselectivity could also be explained by product epimerization during the reaction; however, no epimerization was observed when product **3a** was subjected to the comparable reaction conditions.

In order to gain better understanding of the stereodetermining C–C bond forming step in the proposed mechanism with acridinium-based photocatalyst DFT calculations were performed on the

M062X-D3/6-311+G(d,p) level of theory (see the Supporting Information for details). First, the structure of the sulfinyl imine radical acceptor **1** was evaluated. Previously, Alemán and co-workers tentatively suggested an *s-cis* conformation around the N–S bond as being more stable in this compound due to the hydrogen bonding between the imine proton and the sulfoxide oxygen (Figure 3).¹² Such a conformational preference would then lead to the α -(*R*) product when the *S*(*R*)-sulfinyl imine is employed as the radical acceptor. This stereochemical outcome was indeed observed for both Alemán's and our catalytic system. The calculations confirmed that the *s-cis* conformer is more stable compared to the *s-trans* by 3.8 kcal/mol, corresponding to >99.8:0.2 ratio between the conformers from the Boltzmann distribution at room temperature. In the *s-cis* conformer the expected constructive orbital overlap was observed between the imine hydrogen and the sulfoxide oxygen, while for the *s-trans* conformer the constructive, but weaker, orbital overlap was found between the imine hydrogen and the carbonyl oxygen of the ester group (for a detailed discussion, see the Supporting Information).

Subsequently, the radical addition step was evaluated with the *tert*-butyl radical donor producing product **3a**, and the computed Gibbs free energy diagram for the reaction is presented in Figure 3. The formation of (*R,R*)-diastereomer of **3a** was found to be favored both kinetically and thermodynamically and the computed activation barrier was found to be 3.8 kcal/mol smaller for the *re*-addition compared to the *si*-addition, while the (*R,R*)-diastereomer product is 2.5 kcal/mol more stable compared to the (*R,S*)-diastereomer. The better stabilization of the *re*-TS is in part due to the stronger hydrogen bonding between the imine hydrogen and the sulfoxide oxygen for this transition state, as evident from the calculated bond distances and the visualized molecular orbitals (Figure S3). Additionally, significant sterical crowding occurs in the *si*-TS, where the incoming *tert*-butyl radical requires the mesityl group to become almost completely coplanar to the sulfoxide S=O bond. In contrast, the mesityl group and the S=O bond in the *re*-TS are out of plane by 50° while the incoming *tert*-butyl radical experiences no sterical crowding (Figure 3).

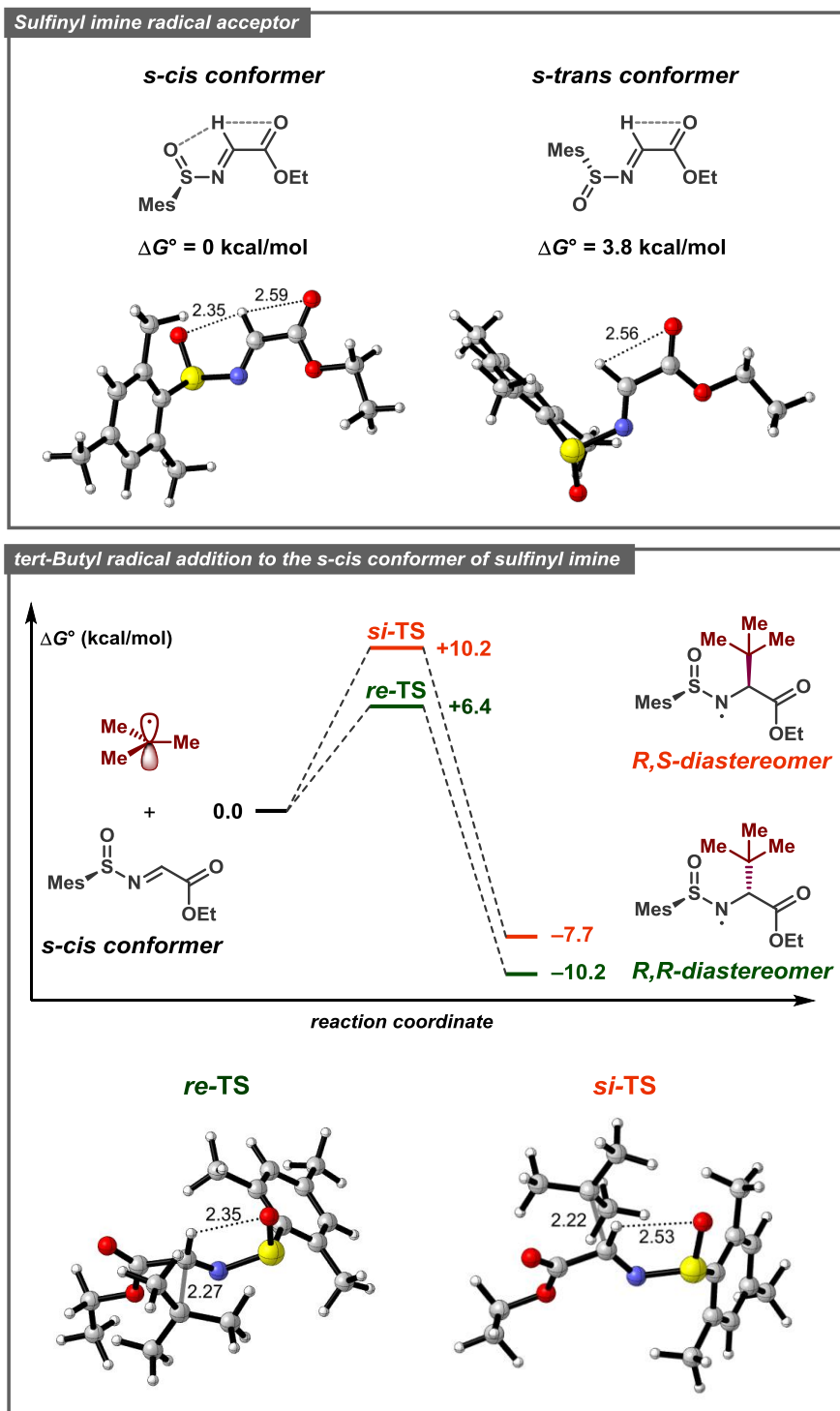


Figure 3. Calculated structures with selected bond distances (Å) for the *s-cis* and *s-trans* isomers of sulfinyl imine **1** (*top*), Gibbs free energy diagram for *tert*-butyl radical addition to **1** (*middle*), and calculated structures for the *re*-TS and *si*-TS transition states (*bottom*).

Conclusions

A practical protocol for stereoselective synthesis of various α -amino acids has been developed, employing ubiquitous carboxylic acids as radical precursors and an organic photocatalyst under visible light irradiation. This protocol allows for synthesis of highly functionalized α -amino acids, which are challenging to prepare through traditional two-electron reaction manifolds. The protocol utilizes near-stoichiometric amounts of reagents and does not produce large quantities of waste, which is an intrinsic disadvantage of the previously described systems utilizing redox-active esters as radical precursors.

ORCID

Andrey Shatskiy: 0000-0002-7249-7437

Anton Axelsson: 0000-0003-0899-2852

Björn Blomkvist: 0000-0001-6026-1921

Jian-Quan Liu: 0000-0002-5533-2075

Peter Dinér: 0000-0001-6782-6622

Markus D. Kärkäs: 0000-0002-6089-5454

Notes

The authors declare no competing financial interest.

Acknowledgements

Financial support from KTH Royal Institute of Technology to M.D.K. is gratefully acknowledged. The Olle Engkvists Stiftelse and the Wenner-Gren Foundations are kindly acknowledged for postdoctoral fellowships to A.S. and J.L., respectively. P.D. acknowledges financial support from the Carl Trygger Foundation for a postdoctoral fellowship to A.A.

References

- (1) (a) Ravikumar, Y.; Nadarajan, S. P.; Yoo, T. H.; Lee, C.; Yun, H. Unnatural Amino Acid Mutagenesis-Based Enzyme Engineering. *Trends in Biotechnology* **2015**, *33*, 462–470. (b) Blaskovich, M. A. T. Unusual Amino Acids in Medicinal Chemistry. *J. Med. Chem.* **2016**, *59*, 10807–10836. (c) Neumann-Staubitz, P.; Neumann, H. The Use of Unnatural Amino Acids to Study and Engineer Protein Function. *Current Opinion in Structural Biology* **2016**, *38*, 119–128.
- (2) Arora, P. K.; Chauhan, A. ACE Inhibitors: A Comprehensive Review. *International Journal of Pharmaceutical Sciences and Research* **2013**, *3*, 532–549.
- (3) De Clercq, E.; Li, G. Approved Antiviral Drugs over the Past 50 Years. *Clinical Microbiology Reviews* **2016**, *29*, 695–747.
- (4) (a) Miller, L. M.; Pritchard, J. M.; Macdonald, S. J. F.; Jamieson, C.; Watson, A. J. B. Emergence of Small-Molecule Non-RGD-Mimetic Inhibitors for RGD Integrins. *J. Med. Chem.* **2017**, *60*, 3241–3251. (b) Giraud, I.; Rapp, M.; Maurizis, J.-C.; Madelmont, J.-C. Synthesis and in vitro Evaluation of Quaternary Ammonium Derivatives of Chlorambucil and Melphalan, Anticancer Drugs Designed for the Chemotherapy of Chondrosarcoma. *J. Med. Chem.* **2002**, *45*, 2116–2119. (c) Ankersen, M.; Johansen, N. L.; Madsen, K.; Hansen, B. S.; Raun, K.; Nielsen, K. K.; Thøgersen, H.; Hansen, T. K.; Peschke, B.; Lau, J.; Lundt, B. F.; Andersen, P. H. A New Series of Highly Potent Growth Hormone-Releasing Peptides Derived from Ipamorelin. *J. Med. Chem.* **1998**, *41*, 3699–3704.
- (5) (a) Gordon, D. E.; Jang, G. M.; Bouhaddou, M.; Xu, J.; Obernier, K.; O’Meara, M. J.; Guo, J. Z.; Swaney, D. L.; Tummino, T. A.; Huettenhain, R.; Kaake, R. M.; Richards, A. L.; Tutuncuoglu, B.; Foussard, H.; Batra, J.; Haas, K.; Modak, M.; Kim, M.; Haas, P.; Polacco, B. J.; Braberg, H.; Fabius, J. M.; Eckhardt, M.; Soucheray, M.; Bennett, M. J.; Cakir, M.; McGregor, M. J.; Li, Q.; Naing, Z. Z. C.; Zhou, Y.; Peng, S.; Kirby, I. T.; Melnyk, J. E.; Chorba, J. S.; Lou, K.; Dai, S. A.; Shen, W.; Shi, Y.; Zhang, Z.; Barrio-Hernandez, I.; Memon, D.; Hernandez-Armenta, C.; Mathy, C. J. P.; Perica, T.; Pilla, K. B.; Ganesan, S. J.; Saltzberg, D. J.; Ramachandran, R.; Liu, X.; Rosenthal, S. B.; Calviello,

- L.; Venkataramanan, S.; Liboy-Lugo, J.; Lin, Y.; Wankowicz, S. A.; Bohn, M.; Sharp, P. P.; Trenker, R.; Young, J. M.; Cavero, D. A.; Hiatt, J.; Roth, T. L.; Rathore, U.; Subramanian, A.; Noack, J.; Hubert, M.; Roesch, F.; Vallet, T.; Meyer, B.; White, K. M.; Miorin, L.; Rosenberg, O. S.; Verba, K. A.; Agard, D.; Ott, M.; Emerman, M.; Ruggero, D.; García-Sastre, A.; Jura, N.; von Zastrow, M.; Taunton, J.; Ashworth, A.; Schwartz, O.; Vignuzzi, M.; d'Enfert, C.; Mukherjee, S.; Jacobson, M.; Malik, H. S.; Fujimori, D. G.; Ideker, T.; Craik, C. S.; Floor, S.; Fraser, J. S.; Gross, J.; Sali, A.; Kortemme, T.; Beltrao, P.; Shokat, K.; Shoichet, B. K.; Krogan, N. J. A SARS-CoV-2-Human Protein-Protein Interaction Map Reveals Drug Targets and Potential Drug-Repurposing. *bioRxiv* **2020**, DOI:10.1101/2020.03.22.002386. (b) Zhang, L.; Lin, D.; Sun, X.; Curth, U.; Drosten, C.; Sauerhering, L.; Becker, S.; Rox, K.; Hilgenfeld, R. Crystal Structure of SARS-CoV-2 Main Protease Provides a Basis for Design of Improved α -Ketoamide Inhibitors. *Science* **2020**, DOI:10.1126/science.abb3405. (c) Zhang, L.; Lin, D.; Kusov, Y.; Nian, Y.; Ma, Q.; Wang, J.; von Brunn, A.; Leyssen, P.; Lanko, K.; Neyts, J.; de Wilde, A.; Snijder, E. J.; Liu, H.; Hilgenfeld, R. α -Ketoamides as Broad-Spectrum Inhibitors of Coronavirus and Enterovirus Replication: Structure-Based Design, Synthesis, and Activity Assessment. *J. Med. Chem.* **2020**, DOI: 10.1021/acs.jmedchem.9b01828. (d) Liu, C.; Zhou, Q.; Li, Y.; Garner, L. V.; Watkins, S. P.; Carter, L. J.; Smoot, J.; Gregg, A. C.; Daniels, A. D.; Jervey, S.; Albaiu, D. Research and Development on Therapeutic Agents and Vaccines for COVID-19 and Related Human Coronavirus Diseases. *ACS Cent. Sci.* **2020**, *6*, 315–331.
- (6) (a) Nájera, C.; Sansano, J. M. Catalytic Asymmetric Synthesis of α -Amino Acids. *Chem. Rev.* **2007**, *107*, 4584–4671. (b) Liu, J.-Q.; Shatskiy, A.; Matsuura, B. S.; Kärkäs, M. D. Recent Advances in Photoredox Catalysis Enabled Functionalization of α -Amino Acids and Peptides: Concepts, Strategies and Mechanisms. *Synthesis* **2019**, *51*, 2759–2791. (c) Ma, J.-A. Recent Developments in the Catalytic Asymmetric Synthesis of α - and β -Amino Acids. *Angew. Chem., Int. Ed.* **2003**, *42*, 4290–4299.

- (7) Eftekhari-Sis, B.; Zirak, M. α -Imino Esters in Organic Synthesis: Recent Advances. *Chem. Rev.* **2017**, *117*, 8326–8419.
- (8) (a) Weix, D. J. Methods and Mechanisms for Cross-Electrophile Coupling of Csp^2 Halides with Alkyl Electrophiles. *Acc. Chem. Res.* **2015**, *48*, 1767–1775. (b) Gandeepan, P.; Müller, T.; Zell, D.; Cera, G.; Warratz, S.; Ackermann, L. 3d Transition Metals for C–H Activation. *Chem. Rev.* **2019**, *119*, 2192–2452. (c) Kaga, A.; Chiba, S. Engaging Radicals in Transition Metal-Catalyzed Cross-Coupling with Alkyl Electrophiles: Recent Advances. *ACS Catal.* **2017**, *7*, 4697–4706. (d) Milan, M.; Salamone, M.; Costas, M.; Bietti, M. The Quest for Selectivity in Hydrogen Atom Transfer Based Aliphatic C–H Bond Oxygenation. *Acc. Chem. Res.* **2018**, *51*, 1984–1995.
- (9) For leading reviews on organic electrocatalysis, see: (a) Shatskiy, A.; Lundberg, H.; Kärkäs, M. D. Organic Electrocatalysis: Applications in Complex Molecule Synthesis. *ChemElectroChem* **2019**, *6*, 4067–4092. (b) Möhle, S.; Zirbes, M.; Rodrigo, E.; Gieshoff, T.; Wiebe, A.; Waldvogel, S. R. Modern Electrochemical Aspects for the Synthesis of Value-Added Organic Products. *Angew. Chem., Int. Ed.* **2018**, *57*, 6018–6041. (c) Yan, M.; Kawamata, Y.; Baran, P. S. Synthetic Organic Electrochemical Methods Since 2000: On the Verge of a Renaissance. *Chem. Rev.* **2017**, *117*, 13230–13319. (d) Kärkäs, M. D. Electrochemical Strategies for C–H Functionalization and C–N Bond Formation. *Chem. Soc. Rev.* **2018**, *47*, 5786–5865.
- (10) For leading reviews on photoredox catalysis, see: (a) Shaw, M. H.; Twilton, J.; MacMillan, D. W. C. Photoredox Catalysis in Organic Chemistry. *J. Org. Chem.* **2016**, *81*, 6898–6926. (b) Kärkäs, M. D.; Porco Jr, J. A.; Stephenson, C. R. J. Photochemical Approaches to Complex Chemotypes: Applications in Natural Product Synthesis. *Chem. Rev.* **2016**, *116*, 9683–9747. (c) Romero, N. A.; Nicewicz, D. A. Organic Photoredox Catalysis. *Chem. Rev.* **2016**, *116*, 10075–10166.
- (11) (a) Wu, G.; Wang, J.; Liu, C.; Sun, M.; Zhang, L.; Ma, Y.; Cheng, R.; Ye, J. Transition Metal-Free, Visible-Light-Mediated Construction of α,β -Diamino Esters via Decarboxylative Radical Addition at Room Temperature. *Org. Chem. Front.* **2019**, *6*, 2245–2249. (b) Yoshimi, Y.; Kobayashi, K.; Kamakura, H.; Nishikawa, K.; Haga, Y.; Maeda, K.; Morita, T.; Itou, T.; Okada, Y.; Hatanaka, M.

- Addition of Alkyl Radicals, Generated from Carboxylic Acids via Photochemical Decarboxylation, to Glyoxylic Oxime Ether: A Mild and Efficient Route to α -Substituted α -Aminoesters. *Tetrahedron Lett.* **2010**, *51*, 2332–2334.
- (12) Garrido-Castro, A. F.; Choubane, H.; Daaou, M.; Maestro, M. C.; Alemán, J. Asymmetric Radical Alkylation of *N*-Sulfinimines under Visible Light Photocatalytic Conditions. *Chem. Commun.* **2017**, *53*, 7764–7767.
- (13) For selected reviews on the use of chiral sulfoxides in asymmetric synthesis, see: (a) Han, J.; Soloshonok, V. A.; Klika, K. D.; Drabowicz, J.; Wzorek, A. Chiral Sulfoxides: Advances in Asymmetric Synthesis and Problems with the Accurate Determination of the Stereochemical Outcome. *Chem. Soc. Rev.* **2018**, *47*, 1307–1350. (b) Carreño, M. C.; Hernández-Torres, G.; Ribagorda, M.; Urbano, A. Enantiopure Sulfoxides: Recent Applications in Asymmetric Synthesis. *Chem. Commun.* **2009**, 6129–6144.
- (14) Ni, S.; Garrido-Castro, A. F.; Merchant, R. R.; deGruyter, J. N.; Schmitt, D. C.; Mousseau, J. J.; Gallego, G. M.; Yang, S.; Collins, M. R.; Qiao, J. X.; Yeung, K.-S.; Langley, D. R.; Poss, M. A.; Scola, P. M.; Qin, T.; Baran, P. S. A General Amino Acid Synthesis Enabled by Innate Radical Cross-Coupling. *Angew. Chem., Int. Ed.* **2018**, *57*, 14560–14565.
- (15) Yoshimi, Y. Photoinduced Electron Transfer-Promoted Decarboxylative Radical Reactions of Aliphatic Carboxylic Acids by Organic Photoredox System. *J. Photochem. Photobiol. A: Chemistry* **2017**, *342*, 116–130.
- (16) Chu, L.; Ohta, C.; Zuo, Z.; MacMillan, D. W. C. Carboxylic Acids as a Traceless Activation Group for Conjugate Additions: A Three-Step Synthesis of (\pm)-Pregabalin. *J. Am. Chem. Soc.* **2014**, *136*, 10886–10889.
- (17) Shang, T.-Y.; Lu, L.-H.; Cao, Z.; Liu, Y.; He, W.-M.; Yu, B. Recent Advances of 1,2,3,5-Tetrakis(carbazol-9-yl)-4,6-dicyanobenzene (4CzIPN) in Photocatalytic Transformations. *Chem. Commun.* **2019**, *55*, 5408–5419.

- (18) Margrey, K. A.; Nicewicz, D. A. A General Approach to Catalytic Alkene Anti-Markovnikov Hydrofunctionalization Reactions via Acridinium Photoredox Catalysis. *Acc. Chem. Res.* **2016**, *49*, 1997–2006.
- (19) (a) Huang, W.; Ye, J.-L.; Zheng, W.; Dong, H.-Q.; Wei, B.-G. Radical Migration–Addition of *N*-tert-Butanesulfinyl Imines with Organozinc Reagents. *J. Org. Chem.* **2013**, *78*, 11229–11237. (b) Matos, J.L.M.; Vásquez-Céspedes, S.; Gu, J.; Oguma, T.; Shenvi, R.A. Branch-Selective Addition of Unactivated Olefins into Imines and Aldehydes. *J. Am. Chem. Soc.* **2018**, *140*, 16976–16981.
- (20) (a) Kammer, L. M.; Rahman, A.; Opatz, T. A Visible Light-Driven Minisci-Type Reaction with *N*-Hydroxyphthalimide Esters. *Molecules* **2018**, *23*, 764. (b) Davies, J.; Angelini, L.; Alkhalifah, M. A.; Malet Sanz, L.; Sheikh, N. S.; Leonori, D. Photoredox Synthesis of Arylhydroxylamines from Carboxylic Acids and Nitrosoarenes. *Synthesis* **2018**, *50*, 821–830.
- (21) (a) Viso, A.; Fernández de la Pradilla, R.; García, A.; Flores, A. α,β -Diamino Acids: Biological Significance and Synthetic Approaches. *Chem. Rev.* **2005**, *105*, 3167–3196. (b) Wang, J.; Zhang, L.; Jiang, H.; Liu, H. Most Efficient Routes for the Synthesis of α,β -Diamino Acid-Derived Compounds. *Current Pharmaceutical Design* **2010**, *16*, 1252–1259.
- (22) Fernández-Salas, J. A.; Maestro, M. C.; Rodríguez-Fernández, M. M.; García-Ruano, J. L.; Alonso, I. Intermolecular Alkyl Radical Additions to Enantiopure *N*-tert-Butanesulfinyl Aldimines. *Org. Lett.* **2013**, *15*, 1658–1661.
- (23) Note, that the excited state of the acridinium photocatalyst is a biradical and is better represented as $\text{Acr}^{\bullet}-\text{Mes}^{\bullet*}$, see the following paper for details: Fukuzumi, S.; Ohkubo, K. Organic Synthetic Transformations Using Organic Dyes as Photoredox Catalysts. *Org. Biomol. Chem.* **2014**, *12*, 6059–6071.
- (24) (a) Uraguchi, D.; Kinoshita, N.; Kizu, T.; Ooi, T. Synergistic Catalysis of Ionic Brønsted Acid and Photosensitizer for a Redox Neutral Asymmetric α -Coupling of *N*-Arylaminomethanes with Aldimines. *J. Am. Chem. Soc.* **2015**, *137*, 13768–13771. (b) Kizu, T.; Uraguchi, D.; Ooi, T.

Independence from the Sequence of Single-Electron Transfer of Photoredox Process in Redox-Neutral Asymmetric Bond-Forming Reaction. *J. Org. Chem.* **2016**, *81*, 6953–6958.